Received August 19, 2020, accepted September 7, 2020, date of publication September 18, 2020,
date of current version September 30, 2020.

Digital Object Identifier 10.1109/ACCESS.2020.3025150

Analysis of Electrical Impedance Myography Electrodes Configuration for Local Muscle Fatigue Evaluation Based on Finite Element Method

DONGMING LI[1,2], LINNAN HUANG[1,2], YANGRONG WEN[1,2], YUEMING GAO[1,2], (Member, IEEE), ŽELJKA LUČEV VASIĆ[3], (Member, IEEE), MARIO CIFREK[3], (Senior Member, IEEE), AND MIN DU[1,4]

[1]College of Physics and Information Engineering, Fuzhou University, Fuzhou 350116, China
[2]Key Laboratory of Medical Instrumentation and Pharmaceutical Technology, Fuzhou 350116, China
[3]Faculty of Electrical Engineering and Computing, University of Zagreb, 10000 Zagreb, Croatia
[4]Key Laboratory of Eco-Industrial Green Technology of Fujian Province, Wuyi University, Nanping 354300, China

Corresponding author: Yueming Gao (fzugym@gmail.com)

This work was supported in part by the National Natural Science Foundation of China under Grant U1505251, and in part by the Project of S&T Department of Fujian Province under Grant 2018I0011.

ABSTRACT Local muscle fatigue (LMF) is a common physiological phenomenon that occurs in daily exercise training and medical rehabilitation. Without timely treatment it can easily lead to muscle spasm, ligament rupture, and even stress fractures. Electrical impedance myography (EIM) is a noninvasive bioelectrical impedance technique suitable for the wearable LMF monitoring anytime and anywhere. In this paper, a novel EIM electrode configuration was proposed by establishing a four-layer simulation model of the human upper arm in FEM software. Sensitivity parameters were introduced to optimize muscle selectivity. The effect of fat thickness on impedance change rate was explored to reduce the influence of individual fat differences on EIM results. Dynamic and static contraction experiments of muscle fatigue were performed on the biceps brachii muscles of 10 volunteers to verify the effectiveness and feasibility of the proposed electrode configuration. The proposed electrode configuration reduced the measurement area by 25%, whereas the impedance amplitude and sensitivity remained the same. The influence of individual fat differences on EIM results was significantly reduced. When the fat thickness increased from 6 mm to 18 mm, the impedance change decreased by 31.78% compared with the traditional electrode configuration. When the muscles were extremely exhausted, the decrease in resistance varied around 10 Ω and within 10^{-1} order of magnitude in different volunteers. In a word, the proposed electrode configuration effectively evaluated the degree of LMF, providing more feasibility for the design of wearable devices.

INDEX TERMS Electrical impedance myography, local muscle fatigue, optimized electrode configurations, finite element method, the biceps brachii muscles.

I. INTRODUCTION

Causes of local muscle fatigue (LMF) often occur in daily life, such as repetitive lifting, carrying, long-term static posture [1], [2], periodic muscle training, and high-intensity rehabilitation actions. LMF is a comprehensive physiological phenomenon that is manifests when the muscle motor system cannot maintain the expected intensity required for a particular action due to the weakening of its functional ability [3]. In general, the physiological LMF is reversible, and muscle blood circulation can be encouraged to recover through relaxation, massage, physical therapy, and other measures. However, if treatment is not given in time, local muscle spasm may occurs [4], [5]. Muscle fibers are separated and broken, resulting in muscle injury and stress fractures when the LMF becomes serious, which in turn would have a severe impact on people's health and quality of life [6]. Therefore, research on wearable devices that can effectively monitor and evaluate LMF anytime and anywhere is of great importance for improving work efficiency, scientific fitness, and accurate rehabilitation.

In a previous study [7] it was suggested that proper electrode configuration can reduce the influence of subcutaneous fat thickness, muscle size, and conductivity on EIM

The associate editor coordinating the review of this manuscript and approving it for publication was Noor Zaman.

impedance value. In another study [8] it was found that the contribution of muscle layer to surface EIM value varies greatly depending on electrode configurations and fat thickness values. However, the existing research is limited to the surface EIM (sEIM) [9], whose impedance value is derived from the contribution of countless tiny areas, such as fat, skin, and bone. Therefore, scientists have introduced finite element modeling (FEM) or finite difference time domain method (FTDT) to perform a ''sensitivity'' analysis on human tissues or organs to determine the impedance values of all conductive tissues inside to select the optimal configuration mode of surface electrodes to improve the selectivity and sensitivity to the target area [8]. Benjamin Sanchez *et al.* introduce model component analysis (MCA) to separate the impedivity of subcutaneous fat and muscle tissues from sEIM data [9]. In one study [10] a finite element model for healthy bodies based on Visible Human Project (VHP) was created and analyzed the positive and negative sensitivity regions in the model were analyzed to empirically verify the designed electrode method designed empirically. In another study [8], the finite element model was compared with human tissue for sensitivity analysis. Different electrode configurations change the sensitivity distribution of layered tissues. Our group measured the impedance change of muscle using the traditional EIM electrode configuration method and evaluated the fatigue state of local muscle based on the change of electrical impedance [9]. The existing EIM electrode configuration method is used in the detection of clinical diseases and its effect is clinically recognized, but it is limited to clinical practice. Therefore, a suitable electrode configuration method for daily motion detection must be found.

Previous EIM analyses had the following limitations. 1) Most of the EIM electrode configuration methods used in the clinic are serial electrode distribution methods [11], which occupy a large area and cannot be easily integrated into wearable devices. 2) The reliability and sensitivity of EIM are affected by the configuration of the surface electrodes. However, current optimization of EIM electrodes focuses on reducing the influence of different fat thicknesses on EIM measurements [12] while neglecting the optimization of the muscle layer percentage contribution to EIM measurements.

The aim of this paper was to present a new method of electrode configuration that reduces the total area occupied and reduces individual fat differences provided that the EIM parameters meet the requirements of wearable devices. We developed a four-layer upper arm geometric model that includes bone, fat, muscle, and skin tissues. Then, the sensitivity analysis method was used to optimize the muscle layer selectivity and the rate of change of EIM impedance with fat thickness was studied to reduce the influence of individual fat differences on EIM results, thus obtaining the optimal electrode configuration method. Finally, the EIM electrode optimization configuration method obtained by simulation was used in dynamic and static *in vivo* experiments on the brachial ends of the volunteers to verify the feasibility of the new electrode configuration method. The results can provide specialized support and theoretical guidance for the development of wearable devices for the evaluation of muscle fatigue.

The rest of this paper is organized as follows. A four-layer arm simulation model for optimization of EIM electrode configuration was described in Section II. Then, we optimize the new electrode configuration by analyzing the sensitivity and rate of EIM impedance change with fat thickness. We used a measurement setup for static and dynamic *in vivo* EIM contraction measurements. The results of the simulation and *in vivo* experiments were presented in Section III. Based on the simulation results and the wearable scenario the optimal electrode configuration was determined. Subsequently, we discussed some related issues and some limitations in Section IV and presented the conclusion of this study.

II. METHODS

The simulation platform was set up using finite element analysis. Based on the simulation platform, the influence of two different electrode configurations on the EIM parameter amplitude was investigated. To increase the percentage of muscle tissue contribution to apparent impedance, the sensitivity of each layer was studied. Afterwards, in order to reduce the influence of individual differences caused by different fat thicknesses on the EIM detection results, the variation of the EIM parameter stability with the change of electrode spacing under different fat thickness was investigated. Finally, the feasibility of the proposed electrode configuration was verified by dynamic and static contraction experiments.

A. SIMULATION METHODS

To obtain geometric model parameters, the physiological parameters of 10 volunteers were measured. Body Mass index (BMI), fat rate, muscle rate, bone mass were measured using the PICOOC Latin Smart Body Scale (PICOOC Inc., Beijing, China). The geometric parameters of the arm were measured manually. The following table shows the average and standard deviation of the individual parameters. The Parameters EC, CA, and CB in Table 1 represent the arm circumference of the elbow joint, arm circumference of the biceps brachii, and arm circumference at armpit, respectively.

According to the model parameters, a four-layer concentric cylinder finite element model was constructed in COMSOL software. The AC / DC module we used is mainly used for static and low frequency electromagnetic simulation, which can effectively solve the distribution problem of excitation current in human tissues, and the parameters of the layered tissue model were calculated by using the fat rate, muscle rate, and arm circumference information. According to the model parameters, a four-layer concentric cylinder finite element model was constructed in COMSOL software, as shown in Fig. 1. The skin was thin, and skin thickness was defined as 1.50 mm [13]; there was little difference in skin thickness between individuals [14]. Parameters r_1, r_2, and r_3 were the thickness of bone, muscle, and fat layers, which were 12.93 mm, 27.23 mm, and 6.09 mm, respectively.

TABLE 1. Physiological parameters of volunteers.

Physiological parameters	Volunteers
BMI	21.03±3.61
Fat (%)	20.90%±0.6%
Muscle (%)	75.57%±0.5%
Bone (kg)	2.7±0.38
Elbow to armpit (cm)	22±1.31
CE (cm)	28±1.42
CB (cm)	26.53±1.93
CA (cm)	25.50±2.42

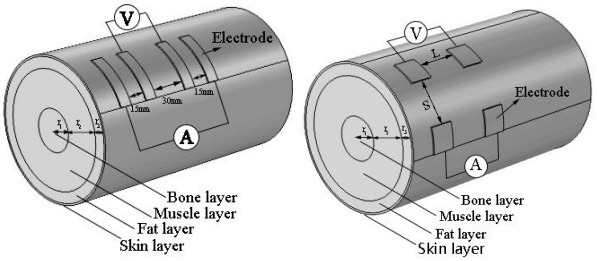

FIGURE 1. A four-layer FEM model of human upper arm: (a) serial electrode configuration method; (b) parallel electrode configuration method.

The current field under AC / DC module is selected in COMSOL to established the electric field model. The electrical characteristic parameters of each layer were imported, including conductivity (σ) and relative dielectric constant (ε). Muscle was set as an anisotropic tissue due to the difference in transverse and longitudinal impedance rates of muscle fibers. The values of transverse and longitudinal electrical parameters were based on the data from Harvard Medical School [15]. Skin, fat, and bone layers were set as isotropic tissues, and their electrical parameters can be found in [16]. In the above-mentioned human upper arm FEM model, the frequency range selected for the EIM research was 10 kHz-1 MHz, which met the requirements of quasi-static approximation [17]. The EIM finite element control equation that conformed to the quasi-static field was expressed by equation (1), as follows [18]:

$$\begin{cases} \nabla \cdot J = Q_j \\ J = (\sigma + j\omega\varepsilon_0\varepsilon)E + J_e \\ E = -\nabla V \end{cases} \tag{1}$$

where J (A/m^2) is the current density, and Q_j(A/m^2) is the total current source, σ (S/m) and ω (rad/s) are the conductivity and angular frequency, respectively, J_e (A/m^2) is the current source density. E (V/m) and V (V) are the electric field strength and potential, respectively. $\sigma(\omega) \in V$ and $\varepsilon_r \in V$ are the conductivity and relative dielectric constant of heterogeneous domain, ε_0 is the vacuum dielectric constant, and $\omega \in V$ is the angular frequency.

To ensure the continuity between layers, the potential and current density continuities were set between each tissue layer of the human upper arm FEM model and between electrodes and skin, as follows [19]–[21]:

$$\begin{cases} V_l = V_{l-1} \\ J_l = J_{l-1} \end{cases} \tag{2}$$

where V_{l-1} and V_l represent the potential values of the adjacent two layers. J_{l-1} and J_l represent the current density values of the adjacent two layers, and the subscript l with values 2, 3, and 4 represents specific tissue layers.

After completion of the construction of the finite element simulation platform according to the measurement principle of EIM, the same excitation current was injected into the muscle mass to be measured. The larger the parameter amplitude and the larger the detection terminal voltage signal, the easier it was to integrate into the wearable device. Therefore, in this section the influence of two different electrode configuration methods on the amplitude of the EIM parameters was analyzed based on the finite element analysis platform.

In Fig. 1 (a) the traditional EIM electrode configuration method is shown. Its four electrodes were arranged in series, with adjacent electrode spacing of 15 mm-30 mm-15 mm and electrode size of 10 mm × 40 mm. In Fig. 1 (b) the newly proposed parallel electrode configuration method is shown. The electrode area was also set to 4 cm^2. To make the muscle mass area approximately equal for both configuration methods, we set L to be 30 mm and S to be 3 mm. Then, we studied the values of the EIM parameter resistance and reactance at four frequency points, namely, 10, 25, 50, and 100 kHz and optimized the positions of the electrodes in this new electrode configuration method using the sensitivity analysis method.

Apparent impedance is the electrical impedance measured on the skin surface. Its value depends on the contribution of each layer below the electrodes, which depends on the electrode characteristics (size, material, shape, and position on the skin). Sensitivity analysis was used to calculate the impedance of each layer and optimize positions of the four electrodes on the skin surface in order to maximize the percentage of muscle tissue contribution to the apparent impedance. The apparent impedance value Z was expressed by Equation (3), as follows:

$$Z = R + jX = Z_p + Z_f + Z_m + Z_b = k(\omega) \int_v \overrightarrow{J^I} \cdot \overrightarrow{J^V} dv \tag{3}$$

where J^{I} and J^{v} are the local current density vectors generated by applying unit currents to the two current electrodes and the two voltage electrodes on the surface, respectively, which can be obtained by the control equation (3) of the FEM. Parameter V refers to the heterogeneous domain V ($V = Vp \cup Vf \cup Vm \cup Vp$), which is composed of four sub-domains

of human tissue. $K(\omega)$ is the impedance rate of the heterogeneous domain [22], and its value is as follows:

$$k(\omega) = \frac{1}{\sigma(\omega) + j\omega\varepsilon_0\varepsilon_r(\omega)} \tag{4}$$

the impedance sensitivity of the four sub-domains of skin, subcutaneous fat, bone, and muscle layers can be calculated using the following formula:

$$\begin{cases} Sen_i = \int_{V_i} \overrightarrow{J^I} \cdot \overrightarrow{J^V} dv \; (i \in p, f, b) \\ Sen_m = Sen_{mT} + Sen_{mL} \\ \quad = \left(\int_{V_m} J_x^I \cdot J_x^V dv + \int_{V_m} J_y^I \cdot J_y^V dv \right) + \int_{V_m} J_z^I \cdot J_z^V dv \end{cases} \tag{5}$$

in equation (5), Sen_{mT} and Sen_{mL} are the transverse sensitivity and longitudinal sensitivity in the muscle layer, respectively. The x and y are the transverse directions of muscle fibers, and z is the longitudinal direction.

We obtained the impedance values of each layer through sensitivity analysis in combination with the control equation of finite element simulation. The parameter sel_{i} is introduced to represent the selectivity of apparent impedance to target region i and is defined as follows:

$$Sel_i = \frac{Z_i}{Z} \approx \frac{R_i}{R} = \frac{\mathrm{Re}\left\{ k_i \int_{V_i} \overrightarrow{J^I} \cdot \overrightarrow{J^V} dv_i \right\}}{\mathrm{Re}\left\{ k \int_V \overrightarrow{J^I} \cdot \overrightarrow{J^V} dv \right\}} \quad (i \in p, f, m, b) \tag{6}$$

where Z_i is the impedance of the target area, Z is the apparent impedance, R_i is the resistance of the target area, R is the apparent resistance, and k_{i} and v_i are the impedance rate and volume of the target area, respectively. k and v are the total impedance rate and the total product, respectively.

The target areas included the skin, fat, muscle, and bone layers. The electrical impedance measured on the skin surface was called apparent impedance, and the proportion of each part in the apparent impedance value changed with the electrode characteristics (size, material, shape, and distribution). The four electrodes on the skin surface were appropriately adjusted to change the sensitivity distribution of subcutaneous layered tissue and to improve the contribution percentage of muscle tissue to apparent impedance.

Based on the finite element simulation platform, we adopted the parallel electrode configuration method and combined the requirements of wearable scenarios to select the appropriate electrode spacing. Two sets of electrode spacings were chosen for sensitivity analysis: $S = 5$ mm, $L = 5$ mm and $S = 20$ mm, $L = 20$ mm, as seen in Fig. 1.

The fat thickness range of healthy human body was selected as follows: 6-18 mm, with 6 mm as the baseline. This baseline was recorded as 1.0 $\times$ and thickened with a step size of 3 mm. The range of muscle size was 30-60 mm; 30 mm is 3.0 $\times$, and the thickness was increased by 10 mm. Then, on the basis of the previous step, the change rule of Sel_{m} with S and L was implemented when the frequency was $f = 50$ kHz, and the fat thickness values were 1.0 $\times$, 1.5 $\times$, and 3.0 $\times$ respectively.

Afterwards, to reduce the influence of individual differences caused by different fat thickness values on the EIM results, the influence of parallel electrode placement on the EIM impedance change rate was evaluate. The degree to which the EIM impedance value was affected by fat thickness was defined as the change rate, represented by β_{fat}, calculated using Equation (7), where Z_{i} and Z_0 are the impedance values before and after the change of fat thickness and muscle size.

$$\beta_{\mathrm{fat}} = \frac{Z_{\mathrm{i}} - Z_0}{Z_0} \times 100\% \tag{7}$$

Similarly, the parallel electrode configuration method was adopted. The variation rule of EIM parameter stability with S and L was explored at a frequency of $f = 50$ kHz and fat thickness values of 1.0 $\times$, 1.5 $\times$, 2.0 $\times$, 2.5 $\times$, and 3.0 $\times$, respectively. When analyzing the influence of spacings S and L on EIM parameters, they were single variables, whereas the other factors were fixed at 5 cm.

B. EXPERIMENTAL METHODS

According to the mechanism of LMF, dynamic and static experimental studies were carried out on the *biceps brachii* muscle of the volunteers using the optimized configuration of EIM electrodes.

Before the LMF weight-bearing experiment, the maximal voluntary contractions (MVC) of each volunteer was measured as the highest load a human arm can hold. MVC was measured in five muscular healthy women (numbered 1-5) and five males (numbered 6-10) with the Biodex System 4. The MVC measurement diagram is shown in Fig. 2, and the basic information and MVC of the volunteers are shown in Table 2.

TABLE 2. MVC data of ten volunteers.

Number	1	2	3	4	5	6	7	8	9
MVC(N·m)	29.6	34.5	37.8	35.6	40.3	56.9	49.9	54.6	58.1

1) STATIC IN VIVO EXPERIMENTAL

Experiments on static muscle contraction were performed to explore the changes of muscle electrical impedance. Before the experiment, the position of the biceps brachii muscle of the human arm was determined. The skin surface was cleaned using cotton with alcohol in order to remove sweat and oil from the skin surface and to improve the adhesion of the electrode to the skin. Then, the electrodes (1 mm thick, 20 mm $\times$ 20 mm in size) were placed directly in the middle of the biceps brachii muscle with a distance of S = 10 mm and L = 20 mm. At the same time, the angle sensor was naturally and evenly fixed on both sides of the elbow joint of the right arm. The acquisition equipment was connected to a computer.

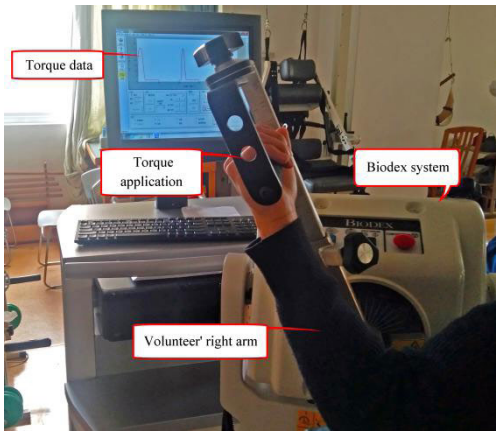

FIGURE 2. MVC measurement diagram.

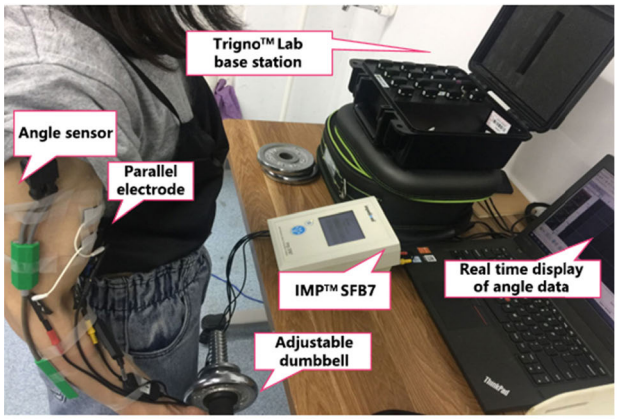

FIGURE 3. EIM experimental platform.

The electrodes were connected to the instrument through an alligator clip of IMPTMSFB7 anthropometric analyzer. The basic information on sex, weight, and height of the volunteers were entered into the instrument, and the EIM impedance value (3 kHz-1 MHz) was measured by choosing the bioelectrical impedance spectrum mode. The measured data were exported to MS Excel form by the supporting software. The in vivo experimental platform is shown in Fig. 3.

A schematic diagram of the static experiment is shown in Fig. 4. During the experiment the angle between upper and lower arms was 135°, as in Fig. 4. Volunteers held dumbbells of different weights (0.1, 0.3, and 0.5 of their MVC) and the EIM impedance values for different load intensities were measured with IMPTMSFB7 anthropometric analyzer. Also, the angle between upper and lower arm was constantly monitored using an angle sensor and the EMGworks software in the computer monitored, in order to avoid changes in muscle length caused by inadvertent angle change or by the sour sensation of the arm during the experiment.

To avoid individual differences in the above mentioned research rules, repeated static experiments were carried out on 10 volunteers.

2) DYNAMIC IN VIVO EXPERIMENTAL

A diagram of the dynamic in vivo experiment is shown in Fig. 5. Using the in vivo experimental platform in Fig. 3,

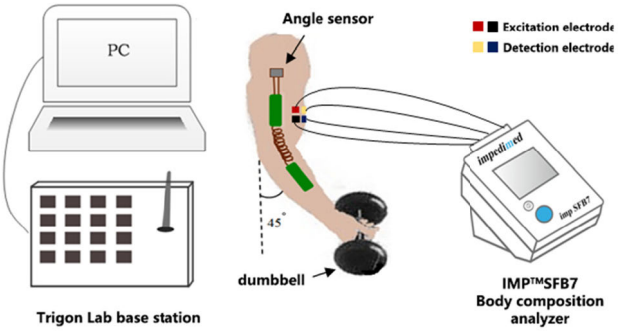

FIGURE 4. Block diagram of static experiment.

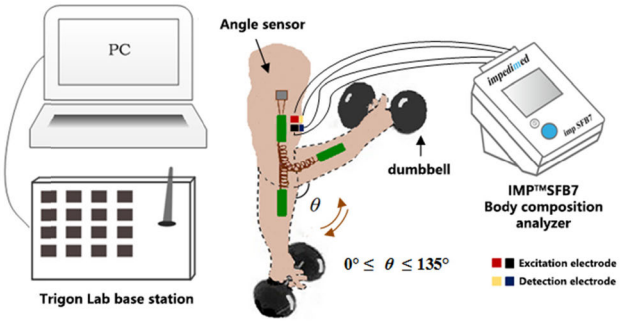

FIGURE 5. Block diagram of dynamic experiment.

volunteers held dumbbells of different weights (0.1, 0.3, and 0.5 MVC) in the right arm and repeatedly performed centripetal and centrifugal movements, as follows: 0°-135° was centripetal contraction and 135°-0° was centrifugal contraction. These angles referred to the angles between the forearm and the vertical plane, as in Fig. 5. The experiment was stopped when the volunteers were completely tired, i.e. the *biceps brachii* muscle showed fatigue, and were unable to continue the intended movement until completion. During the experiment, the impedance characteristics of biceps brachii muscle were tracked with IMPTMSFB7, and the angle sensor was used to monitor the angle.

All the volunteers underwent weight-bearing contraction experiments in batches and were allowed to relax for at least one week between the two consequent contraction experiments, so the endurance of the *biceps brachii* muscle restore to normal level.

Repetitive dynamic experiments were performed on the remaining nine volunteers after the weight-bearing contraction experiments.

III. RESULTS

A. SIMULATION RESULTS

1) RESULTS OF EIM AMPLITUDES PARAMETERS

The measured EIM amplitudes at four frequency points of 10, 25, 50, and 100 kHz were studied for two electrode configurations, serial and parallel, as shown in Table 3.

The initial parallel configuration with electrode spacings of $S = 3$ mm and $L = 30$ mm, with the equal electrode

TABLE 3. EIM parameter amplitude affected by electrode configuration.

Configuration Methods	10 kHz		25 kHz		50 kHz		100 kHz	
	R (Ω)	X (Ω)	R (Ω)	X (Ω)	R (Ω)	X (Ω)	R (Ω)	X (Ω)
Serial Configuration	80.60	16.40	66.82	19.90	56.02	18.80	48.35	11.38
Parallel Configuration	183.70	37.40	164.51	27.60	153.03	20.30	145.50	12.62
Difference	103.10	21.00	97.69	7.7	97.01	1.50	97.15	1.24

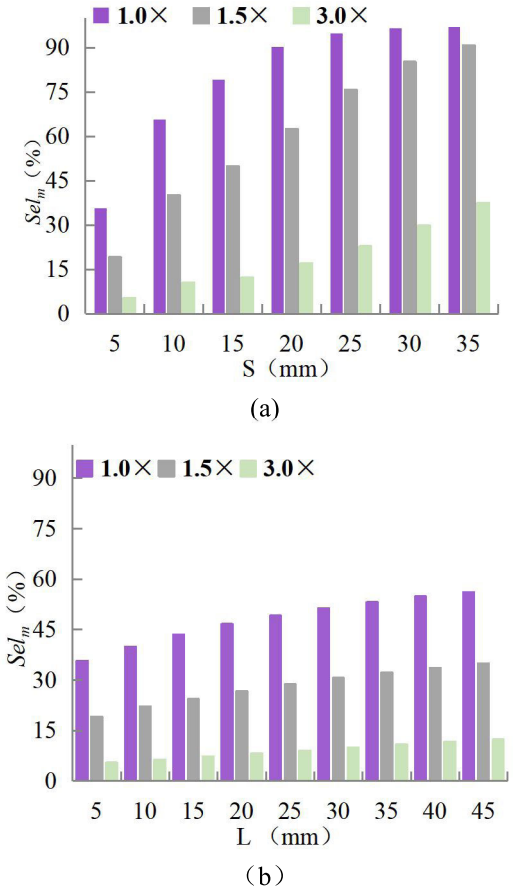

FIGURE 6. (a) The impedance selectivity of EIM varies with S; (b) The impedance selectivity of EIM varies with L.

area as serial configuration and including approximately the same muscle area, resulted in a larger EIM impedance amplitude at all frequencies. The difference was most significant at 10 kHz, with a resistance difference of 103 Ω and a reactance difference of 21 Ω. The larger impedance implies higher detection amplitude, which is easier to integrate into wearable devices. Therefore, the parallel configuration method was preferred in our case.

2) RESULTS OF EIM SELECTIVITY PARAMETERS

Based on the finite element simulation platform, the parallel electrode configuration method was used to analyze the sensitivity of two sets of electrode spacings, namely $S = 5$ mm and $L = 5$ mm and $S = 20$ mm and $L = 20$ mm. The selectivity of apparent impedance to target area i (skin, fat, muscle and bone tissues) was expressed as a percentage. The simulation results are shown in Table 4.

Table 4 shows that the apparent impedance value was formed by superimposing the impedance of different subcutaneous tissues. At 50 kHz, when $S = 5$ mm and $L = 5$ mm, the contribution of the fat layer was 81.05%, and the muscle layer was 19.18%. However, for larger electrode spacing $S = 20$ mm and $L = 20$ mm, the contribution of the fat layer decreased to 28.67%, and the contribution of the muscle layer increased to 71.68%. For the bone and skin layers, the difference was small and changed only within 1%. By adjusting the electrode spacing on the skin surface, the contribution of the muscle tissue is changed in the apparent impedance.

Afterward, the variation rule of the apparent impedance selectivity (Sel_m) to muscle tissue with S and L was studied. The results are shown in Fig. 6.

The selectivity of impedance to muscle tissue Sel_m increased with increasing S and L,and was not influenced by fat thickness. Furthermore, Sel_m increased much faster with increasing S compared to L. Taking the fat thickness of 1.5× as an example, for spacings $L = 5$ mm and $S = 35$ mm, Sel_m was 90.95%, while at $S = 5$ mm and $L = 35$ mm, Sel_m was 32.34%.

3) EXPERIMENTAL RESULTS OF SEMG APPLIED TO MUSCLE FATIGUE

In this section, we investigated the varition of EIM resistance, where S and L increase at a step size of 5 mm at different fat thicknesses. The simulation results are shown in Fig. 7.

Fig. 7 shows that at S = 5 mm and L = 5 mm, the increase of resistance was 236.6% when the fat thickness increased from 1.0 x to 3.0 x. The increase of resistance was 423.3% with increasing fat thickness from 1.0 x to 3.0 x when $L =$ 45 mm. The resistance increased with increasing L and fat thickness, indicating that the resistance stability decreased with increasing L.

At $S = 5$ mm and $L = 5$ mm, the resistance increased 236.66% as the fat thickness increased from 1.0 x to 3.0 x. The increase of resistance was 418.91% with increasing fat thickness from 1.0 x to 3.0 x when $S = 15$ mm and $L =$ 5 mm. Although the resistance change showed a decreasing

TABLE 4. Impedance selectivity affected by electrode configuration.

Impedance(Sel_i)	S = 5 mm, L = 5 mm		S = 20 mm, L = 20 mm	
	50 kHz	100 kHz	50 kHz	100 kHz
Z_{skin} (Sel_s)	-0.22 (-0.28%)	-1.91 (-2.46%)	-0.15 (-0.74%)	-028 (-1.59%)
Z_{fat} (Sel_f)	65.84 (81.05%)	67.44 (86.89%)	5.76 (28.67%)	5.90 (33.64%)
Z_{muscle} (Sel_m)	15.58 (19.18%)	12.05 (15.53%)	14.40 (71.68%)	11.86 (67.62%)
Z_{bone} (Sel_b)	0.04 (0.05%)	0.03 (0.04%)	0.08 (0.39%)	0.06 (0.34%)
$Z_{apparent}$ (Sel)	81.24 (100%)	77.61 (100%)	20.09 (100%)	17.54 (100%)

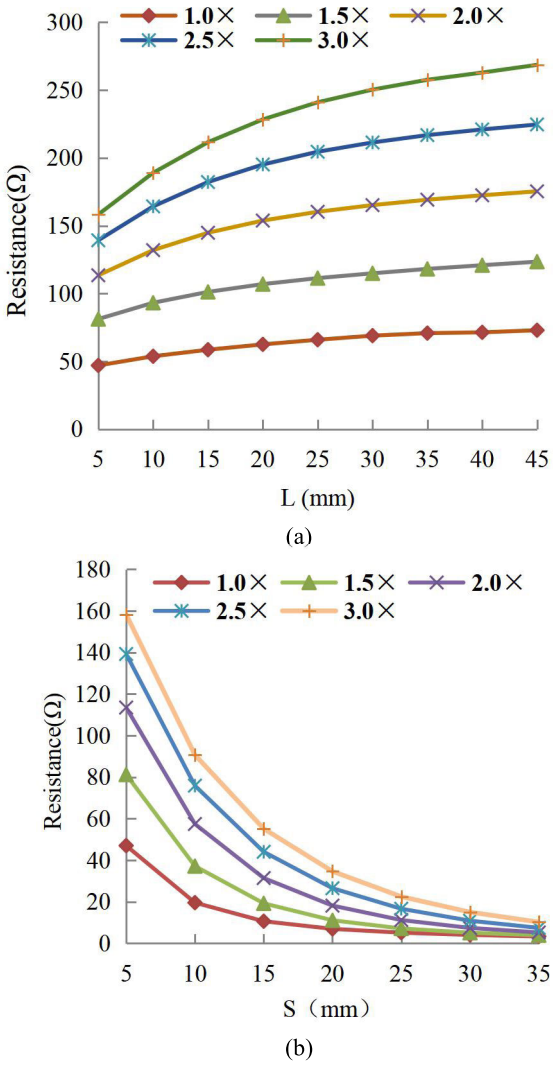

FIGURE 7. (a) The resistance stability of EIM varies with L; (b) The resistance stability of EIM varies with S.

trend with increasing S, the resistance value decreased rapidly and then slowly with increasing S, resulting in an initial increase and later in a decrease of the resistance change.

According to the requirements of the EIM electrode design in this paper, the electrode spacings S and L were selected under comprehensive consideration of the overall occupied area of the electrode, impedance amplitude, stability β_{fat}, and selectivity Sel_{m}. First, we considered Sel_{m}. Fig. 6 shows that at $S = 5$ mm, the maximum value of Sel_{m} was about 50% and the contribution of muscle tissue to apparent impedance was generally small. Therefore, according to Sel_{m}, S should be larger than 5 mm. However, the resistance change rate β_{fat} first increased and then decreased as S increased. At $S = 20$ mm, the rate of change was largest, indicating that stability first decreased and then increased as S increased. Considering the total area occupied by the electrode, $S = 10$ mm was selected. For L, because Sel_{m} increased with L and the rate of change increased with L, $L = 20$ mm was considered a compromise. Therefore, the parallel electrode configuration method with $S = 10$ mm and $L = 20$ mm was finally chosen for the experimental study of LMF. The comparative results obtained with the traditional serial configuration method of 15 mm-30 mm-15 mm are shown in Table 5.

TABLE 5. Comparison of two electrode configurations.

Configuration (mm)	Area (mm^2)	Resistance (Ω)	Change Rate (β_{fat})	*Selectivity* (Sel_m)
15-30-15	4000	35.27-150.15	325.72%	18.15-87.61%
S = 10, L = 20	3000	35.79-140.99	293.94%	16.05-83.70%

As shown in Table 5, at $f = 50$ kHz, the resistance amplitude and Sel_{m} of the two configuration methods did not differ very much, while the parallel configuration method with $S = 10$ mm and $L = 20$ mm showed a 25% smaller total occupied area and a 31.78% lower change rate, corresponding to a 1 mm change in fat thickness, a 3% reduction in change rate, and a 1% lower resistance change.

B. IN VIVO EXPERIMENTAL RESULTS

Based on the mechanism of LMF, dynamic and static in vivo experiments were performed on biceps brachii muscle of volunteers using the optimized configuration of EIM electrodes obtained by simulation in Sction 2.

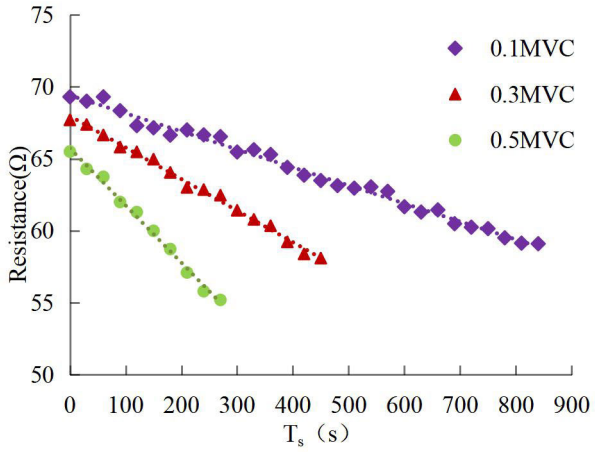

FIGURE 8. Static contraction experiments of muscles under different load conditions (0.1, 0.3, and 0.5 MVC). The down trend of R (50 kHz) in the muscles of Volunteer 1 from complete relaxation to extreme fatigue.

1) STATIC EXPERIMENTAL RESULTS

First, the characteristics of the EIM impedance values during biceps fatigue were examined under three load intensities (0.1, 0.3, and 0.5 MVC). The trend of change in resistance is shown in Fig. 8. T_S was the time taken for the muscle to change from a resting state to a fully fatigued state. When the muscle was in a state of complete fatigue, the EIM impedance value hardly changed.

Fig. 8 shows the following rule. At $f = 50$ kHz the EIM impedance value had a linear correlation with the degree of muscle fatigue, while the resistance had a negative correlation with the degree of fatigue. In addition, for higher MVCs fatigue accumulation was faster, resulting in a higher slope of the linear curve and shorter duration of the experiment T_S. For example, $T_S = 840$ s under 0.1 MVC load, and $T_S = 270$ s under 0.5 MVC load. Moreover, the change amplitude ΔR of the EIM impedance value of the three load levels (0.1, 0.3, and 0.5 MVC) showed only slight differences over time T_S; the resistance reduction ΔR was 10.2, 9.6, and 10.3 Ω, respectively. Preliminary results showed that the degree of muscle fatigue can be determined as a function of the variation amplitude of the EIM impedance value.

To avoid individual differences in the above mentioned research rules, repeated static experiments were performed on 10 volunteers. Fig.9 shows the EIM impedance values and the variation amplitude of the 10 volunteers before and after biceps brachii fatigue under the load capacity of 0.3 MVC.

Fig. 9 shows large differences in the initial EIM impedance values, which depended on the fat level of the volunteers. For thicker fat tissue, the resistance value was higher.

However, hen the muscle was almost exhausted, amplitude of the EIM impedance decreased for almost the same amount for all volunteers. This resistance reduction ΔR was in the range of 9.67-10.62 Ω. These results showed that when the muscle static contraction was close to a complete fatigue, the resistance decreased by about 10 Ω.

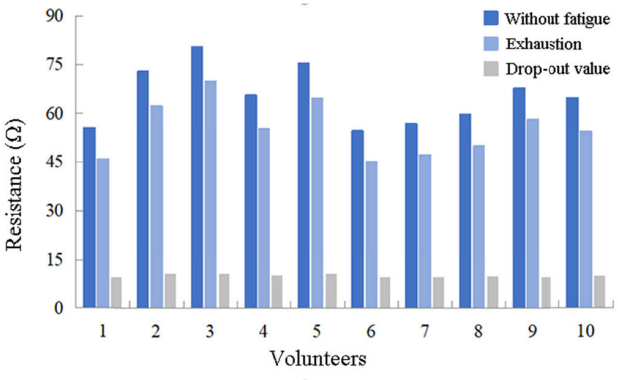

FIGURE 9. Resistance changes of 10 volunteers before and after the static experiment for 0.3 MVC load.

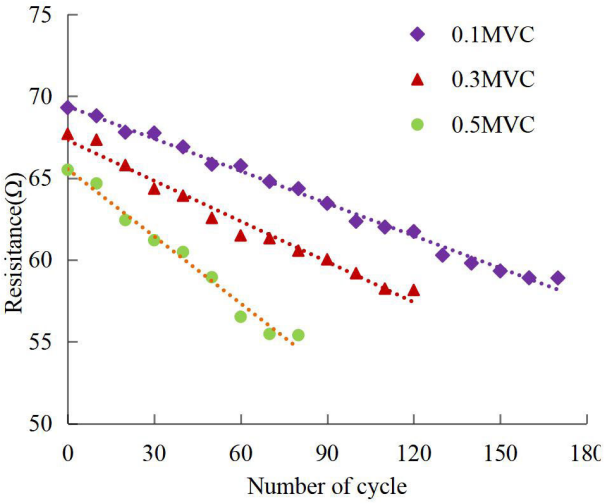

FIGURE 10. Dynamic contraction experiments of muscles under different load conditions (0.1, 0.3, and 0.5 MVC). The decrease of R (50 kHz) in the muscles of volunteer #1 from complete relaxation to extreme fatigue.

2) DYNAMIC EXPERIMENTAL RESULTS

In the dynamic experiment the number of contraction cycles was used to reflect the degree of muscle fatigue, since each contraction cycle contributed to the fatigue of the biceps brachii muscle.

The change of the resistance with the number of contractions measured on the volunteer #1 for three load conditions (0.1, 0.3, and 0.5 MVC) is depicted in Fig. 10.

For all three loads the measured electrical impedance had a linear relationship with the number of contraction cycles, i.e. duration of the experiment, which is consistent with the static experiment results. The resistance was positively correlated with the degree of fatigue, and the reactance was negatively correlated with the degree of fatigue. The biceps brachii was in a completely fatigued exhaustion when the change in the amplitude of the EIM impedance value between two contraction cycles was extremely small and almost constant. The number of dynamic contraction cycles performed by the biceps brachii muscle from the start of the exercise to exhaustion was expressed as Td. Under different loads,

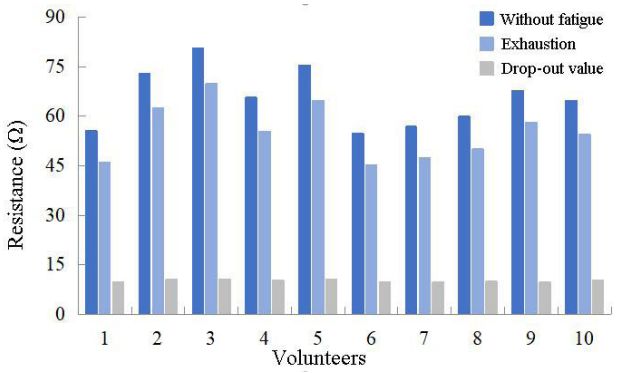

FIGURE 11. Resistance changes of 10 volunteers before and after the dynamic experiment for 0.3 MVC load.

Td values differed: for heavier loads the Td value was shorter, indicating that the volunteer's fatigue progress was faster. For example, under 0.1 MVC load, $T_d = 170$, which was equivalent to 312 s, whereas under 0.5 MVC load, $T_d = 80$, which is equivalent to 147 s. Comparing static and dynamic contraction experiments under the same load conditions, muscle fatigue and exhaustion occurred sooner in a dynamic contraction experiment. In addition, during one exercise with duration T_d, the resistance variations ΔR for different loads were 10.41, 9.54, and 10.1 Ω. To avoid individual differences in the above mentioned research rules, repeated dynamic experiments were performed by the remaining 9 volunteers. The results presented in Fig. 11 were obtained for 0.3 MVC load, and the electrical resistance change ΔR between the beginning and the end of the exhaustion decreased around 10 Ω for different volunteers.

IV. DISCUSSION

EIM method is a non-invasive bioelectrical impedance myography technology based on four electrodes. In EIM, electrical impedance is used to evaluate the tissue characteristics of local muscles or muscle groups. It is an effective tool to detect muscle fatigue. However, serial electrodes configuration method commonly used in clinic for EIM measurements is not suitable for wearable application scenarios and muscle fatigue monitoring in real time. Therefore, an electrode configuration is needed that occupies a small area and with EIM parameters that meet the requirements of wearable devices.

In this paper, a more compact electrodes configuration was presented based on the finite element simulation platform. By optimizing the electrodes positions and spacings, the influence of anatomical factors on the EIM parameter measurement values was minimized and the contribution of the muscle layer to surface EIM impedance was increased, thereby enabling EIM to evaluate muscle state more effectively. The effectiveness of LMF detection was verified by *in vivo* experiments.

In the process of optimizing the electrode configuration, potential distribution and current density achieved in a bone tissue layer were much lower than those in a muscle and fat layers, because the bone was located in the innermost layer of the upper arm model. Therefore, when considering the influence of EIM impedance value on each tissue layer, only muscle and fat layers were considered, since they occupy a large proportion of the upper arm. In addition, due to the small value of reactance in the human body, its influence was also small. Thus, in this paper, in order to improve research efficiency, we considered only the influence of the EIM resistance parameters. However, research on the EIM reactance is also very meaningful, and the values of reactance amplitude and phase are also very important for evaluating EIM method.

During the static contractions experiment performed on the *biceps brachii* muscle, the resistance reduction ΔR at the end of the static experiment varied in the range of 9.67-10.62 Ω. During the dynamic contractions experiment on the *biceps brachii*, the resistance variation ΔR between the beginning and the end of the exercise (exhaustion) varied around 10 Ω within the order of $10^{-2}\Omega$, which was slightly different from that obtained at the end of the static experiment. Therefore, the change in the EIM impedance value did not depend on the type of the movement but was related to the change of the individual's own electrical characteristics.

This paper focused on the electrode spacing in the parallel configuration method but did not deeply explore the influence of electrode material, electrode shape, and electrode size on EIM parameters, which will be done in the future. The configuration proposed in this paper was applied to a *biceps brachii* muscle. However, due to the non-invasiveness and painless characteristics of the EIM method, it is convenient for the evaluation of the fatigue of other muscles, too. For example, application to back muscles can prevent and reduce the possibility of lumbar muscle strain.

V. CONCLUSION

In this paper, a new electrode configuration method suitable for wearable applications was proposed. First, a finite element simulation platform was established, and the effect of individual fat differences on EIM results were explored and reduced. To test its effectiveness in LMF evaluation, muscle fatigue dynamic and static contraction experiments were carried out on *biceps brachii* muscles of 10 volunteers. The results are as follows:

The proposed parallel configuration method can meet the requirements of LMF measurement in wearable scenarios with small size requirements. Compared with the common clinical serial configuration method of 15 mm-30 mm-15mm, the proposed parallel configuration method reduced the total measurement area by 25%. The amplitude of Sel_m and parameters did not differ much from the serial configuration method, and the change rate decreased by 31.78% at $f = 50$ kHz.

The research results can provide technical support and theoretical guidance for evaluating the development of LMF wearable devices. In EIM static experiments, the resistance parameters of different volunteers showed a linear downward

trend, and the resistance values decreased to 10.2, 9.6, and 10.3 Ω under three different loads (0.1, 0.3, and 0.5 MVC), whereas in dynamic experiments, the resistance changes ΔR were 10.41, 9.54, and 10.1 Ω, respectively. In both experiment groups, the resistance change ΔR varied around 10 Ω. For heavier loads the volunteer's fatigue progress was faster and the the EIM resistance parameter decreased faster. Consequently, LMF can be evaluated by the measured decrease in the EIM resistance parameters. In the future work, we intend to separate the impedance characteristics of muscle tissue and other tissue layers from the results of sEIM measurement to improve the sensitivity of detecting changes in muscle impedance.

REFERENCES

[1] S. A. Oyewole, "Enhancing ergonomic safety effectiveness of repetitive job activities: Prediction of muscle fatigue in dominant and nondominant arms of industrial workers," *Hum. Factors Ergonom. Manuf. Service Ind.*, vol. 24, no. 6, pp. 585–600, Nov./Dec. 2014.
[2] J. Bouffard, C. Yang, M. Begon, and J. Côté, "Sex differences in kinematic adaptations to muscle fatigue induced by repetitive upper limb movements," *Biol. Sex Differences*, vol. 9, no. 1, p. 11, Apr. 2018.
[3] A. B. B. Coutinho, B. Jotta, T. S. Carvalho, A. V. Pino, and M. N. Souza, "An alternative electrical impedance myography technique for assessment of local muscular fatigue," in *Proc. Ii Latin Amer. Conf. Bioimpedance*, vol. 54, F. Simini and P. BertemesFilho, Eds. New York, NY, USA: Springer, 2016, pp. 24–27.
[4] N. L. Nelson and J. R. Churilla, "A narrative review of exercise-associated muscle cramps: Factors that contribute to neuromuscular fatigue and management implications," *Muscle Nerve*, vol. 54, no. 2, pp. 177–185, Aug. 2016.
[5] D. Jahic and E. Begic, "Exercise-associated muscle cramp-doubts about the cause," *Materia Socio-Medica*, vol. 30, no. 1, pp. 67–69, 2018.
[6] Q. Wang, X. Cao, G. Yin, and J. Guo, "Evaluation of muscle fatigue process based on ultrasonic image entropy characteristics," *Chin. J. Biomed. Eng.*, vol. 34, no. 1, pp. 30–36, 2015.
[7] M. Jafarpoor, J. Li, J. K. White, and S. B. Rutkove, "Optimizing electrode configuration for electrical impedance measurements of muscle via the finite element method," *IEEE Trans. Biomed. Eng.*, vol. 60, no. 5, pp. 1446–1452, May 2013.
[8] S. B. Rutkove, A. Pacheck, and B. Sanchez, "Sensitivity distribution simulations of surface electrode configurations for electrical impedance myography," *Muscle Nerve*, vol. 56, no. 5, pp. 887–895, Nov. 2017.
[9] H. Kwon, W. Q. Malik, S. B. Rutkove, and B. Sanchez, "Separation of subcutaneous fat from muscle in surface electrical impedance myography measurements using model component analysis," *IEEE Trans. Biomed. Eng.*, vol. 66, no. 2, pp. 354–364, Feb. 2019.
[10] A. A. Danilov, V. K. Kramarenko, and A. S. Yurova, "Modelling of bioimpedance measurements: Application to sensitivity analysis," in *Computational Modeling of Objects Presented in Images: Fundamentals, Methods, and Applications* (Lecture Notes in Computer Science), vol. 8641, Y. J. Zhang and J. Tavares, Eds. Berlin, Germany: Springer-Verlag, 2014, pp. 328–338.
[11] L. Nescolarde, J. Yanguas, J. Terricabras, H. Lukaski, X. Alomar, J. Rosell-Ferrer, and G. Rodas, "Detection of muscle gap by L-BIA in muscle injuries: Clinical prognosis," *Physiol. Meas.*, vol. 38, no. 7, pp. L1–L9, Jun. 2017.
[12] H. Kwon, S. B. Rutkove, and B. Sanchez, "Recording characteristics of electrical impedance myography needle electrodes," *Physiol. Meas.*, vol. 38, no. 9, pp. 1748–1765, Aug. 2017.
[13] X. Zeng, Y. Gao, S. Pan, B. Mai, M. Wei, and M. Du, "Effects of muscle conductivity on signal transmission of intra-body communications," *J. Electron. Meas. Instrum.*, vol. 27, no. 1, pp. 21–25, Nov. 2013.
[14] Y.-M. Gao, H.-F. Zhang, S. Lin, R.-X. Jiang, Z.-Y. Chen, Ž. L. Vasić, M.-I. Vai, M. Du, M. Cifrek, and S.-H. Pun, "Electrical exposure analysis of galvanic-coupled intra-body communication based on the empirical arm models," *Biomed. Eng. OnLine*, vol. 17, no. 1, p. 16, Jun. 2018.
[15] L. L. Wang, M. Ahad, A. McEwan, J. Li, M. Jafarpoor, and S. B. Rutkove, "Assessment of alterations in the electrical impedance of muscle after experimental nerve injury via finite-element analysis," *IEEE Trans. Biomed. Eng.*, vol. 58, no. 6, pp. 1585–1591, Jun. 2011.
[16] S. Gabriel, R. W. Lau, and C. Gabriel, "The dielectric properties of biological tissues: III. parametric models for the dielectric spectrum of tissues," *Phys. Med. Biol.*, vol. 41, no. 11, pp. 2271–2293, Nov. 1996.
[17] K. R. Foster and H. P. Schwan, "Dielectric properties of tissues and biological materials:A critical review," *Crit. Rev. Biomed. Eng., Rev.*, vol. 17, no. 1, pp. 25–104, 1989.
[18] Y. M. Gao, Z. M. Wu, S. H. Pun, P. U. Mak, M. I. Vai, and M. Du, "A novel field-circuit fem modeling and channel gain estimation for galvanic coupling real IBC measurements," *Sensors*, vol. 16, no. 4, p. 15, Apr. 2016.
[19] Y. M. Gao, P. U. Shao-Heng, D. U. Min, V. A. I. Mang-I, and M. A. K. Peng-Un, "Construction and validation of galvanic coupling human intra-body communication model with quasistatic approximation," *Space Med. Med. Eng.*, vol. 22, no. 6, pp. 427–432, 2009.
[20] K. Spitzer, "The three-dimensional DC sensitivity for surface and subsurface sources," *Geophys. J. Int.*, vol. 134, no. 3, pp. 736–746, Sep. 1998.
[21] M. Furche and A. Weller, "Sensitivity distributions of different borehole electrode configurations considering a model with a cylindrical coaxial boundary," *Geophys. J. Int.*, vol. 149, no. 2, pp. 338–348, May 2002.
[22] Y.-M. Gao, Y.-T. Ye, S. Lin, Ž. L. Vasić, M.-I. Vai, M. Du, M. Cifrek, and S.-H. Pun, "Investigation of implantable signal transmission characteristics based on visible data of the human leg," *Biomed. Eng. OnLine*, vol. 16, no. 1, p. 14, Jul. 2017, Art. no. 88.

DONGMING LI received the B.S. degree from the College of Electrical Engineering, Fuzhou University, Fuzhou, China, in 2016, where he is currently pursuing the M.S. degree with the College of Physical and Information Engineering. His current research interests include neural networks and biomedical signal detecting technology.

LINNAN HUANG received the B.S. degree from the College of Optoelectronics and Information Engineering, Fujian Normal University, Fuzhou, China, in 2018. She is currently pursuing the M.S. degree with the College of Physical and Information Engineering, Fuzhou University. Her current research interests include intra-body communication and biomedical signal detecting technology.

YANGRONG WEN received the B.S. degree from the College of Optoelectronics and Information Engineering, Fujian Normal University, Fuzhou, China, in 2018. He is currently pursuing the M.S. degree with the College of Physical and Information Engineering, Fuzhou University. His current research interests include intra-body communication and biomedical signal detecting technology.

YUEMING GAO (Member, IEEE) received the Ph.D. degree in electrical engineering from Fuzhou University, Fuzhou, China, in 2010. He is currently a Professor with the College of Physical and Information Engineering, Fuzhou University. Since 2004, he has been involved in research in the areas of bioelectromagnetism and biomedical signal detecting technology.

ŽELJKA LUČEV VASIĆ (Member, IEEE) received the Dipl.lng. and Ph.D. degrees in electrical engineering from the University of Zagreb, Zagreb, Croatia, in 2007 and 2014, respectively. She is currently an Assistant Professor with the Department of Electronic Systems and Information Processing, Faculty of Electrical Engineering and Computing, University of Zagreb. Her research activities are in the fields of biomedical electronic instrumentation and human-body signal transmission. She is a member of the IFMBE and CROMBES, and serves as the Chair of the IEEE EMB Croatian Section.

MARIO CIFREK (Senior Member, IEEE) received the Dipl.Ing., M.Sc., and Ph.D. degrees in electrical engineering from the Faculty of Electrical Engineering and Computing, University of Zagreb, Zagreb, Croatia, in 1987, 1992, and 1997, respectively, all in electrical engineering. He is currently a Professor of electrical engineering with the Department of Electronic Systems and Information Processing, Faculty of Electrical Engineering and Computing, University of Zagreb. His research interests are focused on the design of biomedical instrumentation and biomedical signal analysis for research and clinical applications. He is a member of the IFMBE, CROMBES, KoREMA, and HMD. Since 2005, he has been a member of the Croatian Academy of Engineering.

MIN DU received the Ph.D. degree in electrical engineering from Fuzhou University, Fuzhou, China, in 2005. Since 2007, she has been the Associate Director of the Key Laboratory of Eco-Industrial Green Technology of Fujian Province, Nanping, China. She is currently a Professor and a Doctoral Supervisor with Fuzhou University. Her research interests include smart instruments and photoelectric.